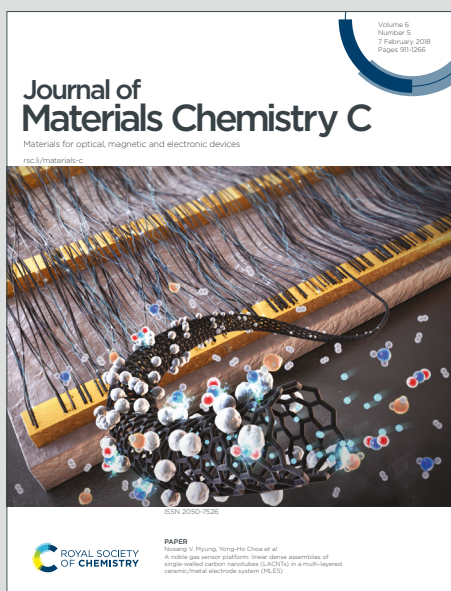


# Journal of Materials Chemistry C

Materials for optical, magnetic and electronic devices

Accepted Manuscript

This article can be cited before page numbers have been issued, to do this please use: J. Tu, Y. Fan, J. Wang, X. Li, F. Liu, M. Han, C. Wang, Q. Li and Z. Li, *J. Mater. Chem. C*, 2019, DOI: 10.1039/C9TC03515J.



This is an Accepted Manuscript, which has been through the Royal Society of Chemistry peer review process and has been accepted for publication.

Accepted Manuscripts are published online shortly after acceptance, before technical editing, formatting and proof reading. Using this free service, authors can make their results available to the community, in citable form, before we publish the edited article. We will replace this Accepted Manuscript with the edited and formatted Advance Article as soon as it is available.

You can find more information about Accepted Manuscripts in the [Information for Authors](#).

Please note that technical editing may introduce minor changes to the text and/or graphics, which may alter content. The journal's standard [Terms & Conditions](#) and the [Ethical guidelines](#) still apply. In no event shall the Royal Society of Chemistry be held responsible for any errors or omissions in this Accepted Manuscript or any consequences arising from the use of any information it contains.

## ARTICLE

## Halogen-substituted triphenylamine derivatives with intense mechanoluminescence property

Received 00th January 20xx,  
Accepted 00th January 20xx

DOI: 10.1039/x0xx00000x

Jin Tu, ‡<sup>a</sup> Yunhao Fan, ‡<sup>a</sup> Jiaqiang Wang,<sup>a</sup> Xiaoyu Li,<sup>a</sup> Fan Liu,<sup>a</sup> Mengmeng Han,<sup>a</sup> Can Wang,<sup>a</sup> Qianqian Li<sup>a</sup> and Zhen Li<sup>\*a,b</sup>

Three triphenylamine (TPA) derivatives, constructed by the introduction of halogen atoms to TPA, show strong mechanoluminescence emissions, partially due to their various electronic configurations by virtue of the electron withdrawing ability of halogen atoms. Careful investigation of their single crystals and the density functional theory (DFT) calculations based on the crystal structure demonstrate that the enhanced intermolecular interactions and twisted molecular structure contribute to their strong ML emission.

## Introduction

Triphenylamine (TPA), a well-known building block, has aroused great attention due to its facile synthesis, flexible modification, excellent electron donating capability and twisted molecular structure.<sup>[1-8]</sup> By introducing different functional groups on TPA, the TPA derivatives have been widely utilized as hole transporting materials or light emitters in organic light-emitting diode (OLED), organic field-effect transistors (OFET), organic solar cells (OSC), non-linear optical (NLO) materials, and so on.<sup>[9-18]</sup> As reported by Li and co-workers, TPA based luminogens, as a superior host in OLED device, exhibited the improved external quantum efficiency of 18.2%, which exceeded that of the device based 4,4'-bis(9H-carbazole-9yl)biphenyl (CBP) (15.7%), for their distinct electronic properties and twisted configuration.<sup>[19]</sup> By utilizing a TPA containing polymer as the hole-transporting material, Zhu and co-workers achieved the highest power conversion efficiencies up to 20.91% in p-i-n planar perovskite solar cells (PVSCs).<sup>[20]</sup>

Mechanoluminescence (ML) first recorded by Francis Bacon in 1605, has received increasing interests in recent few years after a long time of silence, due to their promising applications in the photoelectric fields, including bio-images, pressure sensing, display as well as lighting.<sup>[21-24]</sup> Under the mechanical stimulation, the ML materials could induce light emission

without UV excitation.<sup>[25-26]</sup> Previously, the notorious aggregation-caused quenching (ACQ) effect of luminogens badly restricted the obtaining of strong ML.<sup>[27-28]</sup> Fortunately, the introduction of the twisted structure with the aggregation induced emission (AIE) characteristic or planar  $\pi$  systems with isolated groups could overcome this obstacle, leading to the rapid development of ML luminogens.<sup>[29-34]</sup> And to further investigate the mechanism and configurational relationship of organic ML materials, it is needed to enrich the ML family.<sup>[35]</sup> Considering the twisted molecular structure of TPA block, TPA derivatives could also avoid the undesirable influence of the ACQ effect. Moreover, thanks to the high reaction activity of the TPA moiety, it should be convenient to modify TPA block and develop TPA based ML materials. However, so far, the reported TPA derivatives with intense ML emission were still very scarce (Chart S1).

As presented in the reported ML materials by our group and others, the molecular packing, largely affected by the electronic configuration, is mainly responsible for the ML

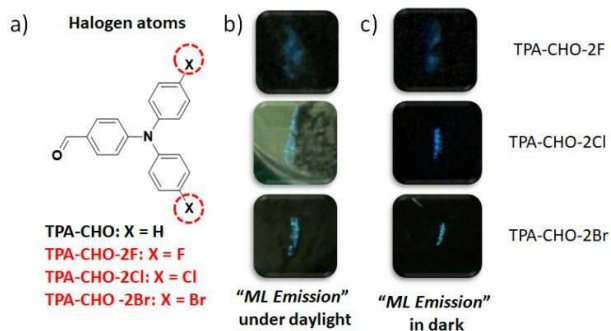


**Fig. 1** a) Chemical structure of TPA derivative, b) ML images of the TPA derivatives under the daylight, c) ML images of TPA-CHO-2X.

<sup>a</sup> Sauvage Center for Molecular Sciences, Department of Chemistry, Wuhan University, Wuhan, 430072, China. E-mail: lizhen@whu.edu.cn, lichemlab@163.com, Fax: +86-27-68755767

<sup>b</sup> Institute of Molecular Aggregation Science, Tianjin University, Tianjin 300072, China.

† Electronic Supplementary Information (ESI) available: [details of any supplementary information available should be included here]. See DOI: 10.1039/x0xx00000x

‡These authors contributed equally.

## ARTICLE

## Journal Name

performance in solid state.<sup>[29-34]</sup> And materials with tight molecular packing could favour the ML emission in solid, since the tight packing can restrain the molecular mechanical movement and mitigate the undesirable energy loss through non-radiative relaxation channels upon a mechanical force. Because of the intimate relationship between the molecular packing and electronic structure, ML performance could be significantly affected by the substituent groups, which could modulate the molecular electronic structure.<sup>[28-36]</sup> Thus, three TPA derivatives were obtained by introducing two halogen atoms (F, Cl, Br) to the non-ML **TPA-CHO** (Fig. 1). Really, upon the linkage of halogen atoms, the electronic structure of **TPA-CHO** was changed, resulting in the tight packing of the halogen-substituted TPA derivatives (**TPA-CHO-2F**, **TPA-CHO-2Cl** and **TPA-CHO-2Br**) accompanied with the appearance of ML emissions. Thanks to their simple structures, it is convenient to explore the structure-packing-performance relationship. Herein, we would like to present their syntheses, structural characterization, photophysical properties, the ML properties, crystal structures, theoretical calculations based on their single crystals, and related discussions on the structure-packing-performance relationship.

## Results and discussion

These three molecules was designed and synthesized according to the route depicted in Scheme S1. All of them were prepared by Ullmann reaction and subsequent Vilsmeier-Haack reaction. Silica gel chromatography was used to purify the target molecules, and their chemical structures were confirmed by <sup>1</sup>H and <sup>13</sup>C NMR spectra (Fig. S1-S8). DSC of those TPA-based molecules were also conducted, **TPA-CHO-2F** and **TPA-CHO-2Cl** showed obvious exothermic peaks, indicating

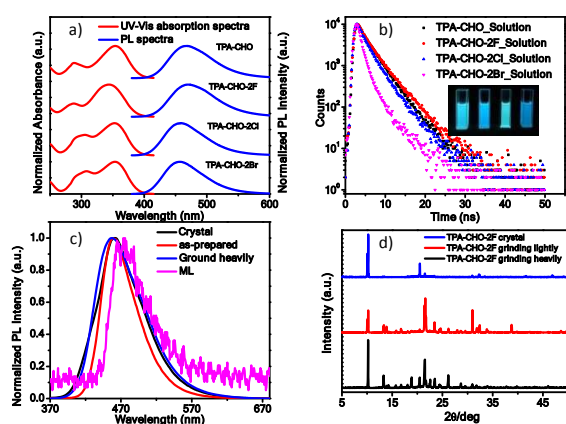


**Fig. 2** a) UV-vis absorption (red line) and PL (blue line) spectra of **TPA-CHO**, **TPA-CHO-2F**, **TPA-CHO-2Cl** and **TPA-CHO-2Br** (Concentration: 10  $\mu$ M) in THF. b) Emission decay of **TPA-CHO**, **TPA-CHO-2F**, **TPA-CHO-2Cl** and **TPA-CHO-2Br** (Concentration: 10  $\mu$ M) in THF. c) PL spectra of **TPA-CHO-2F** before and after grinding in solid state and ML spectra of **TPA-CHO-2F**. d) the XRD patterns of **TPA-CHO-2F**.

**TPA-CHO-2F** and **TPA-CHO-2Cl** possess much enhanced intermolecular interactions (Fig. S9). These TPA derivatives had excellent solubility in common organic solvents, such as tetrahydrofuran (THF), dichloromethane (DCM) and chloroform. UV-Vis absorption spectra of **TPA-CHO**, **TPA-CHO-2F**, **TPA-CHO-2Cl** and **TPA-CHO-2Br** were measured in THF solution (Fig. 2a). All of them possessed the two absorption peaks (centred at 287 and 354 nm for **TPA-CHO**, 287 and 344 nm for **TPA-CHO-2F**, 305 and 353 nm for **TPA-CHO-2Cl**, 308 and 353 nm for **TPA-CHO-2Br**), the bands in the shorter wavelength region were associated with the  $\pi$ - $\pi^*$  transition and the bands in the longer wavelength regions were attributed to the intramolecular charge transfer (ICT). In comparison with those of **TPA-CHO**, **TPA-CHO-2Cl** and **TPA-CHO-2Br**, **TPA-CHO-F** exhibited a slightly blue-shifted absorption bands (about 10 nm), possibly due to the different electron withdrawing properties of halogen atoms. The minor differences in their absorption spectra indicated the different electronic structures caused by the introduction of halogen atoms. The fluorescence emission behaviors of TPA derivatives in solution were also investigated (Fig. 2a), with the results listed in Fig. 1. **TPA-CHO** and **TPA-CHO-2F** exhibited similar emission peaks at about 470 nm in THF solution. For **TPA-CHO-2Cl** and **TPA-CHO-2Br**, minor blue-shifted emission bands were observed (459 and 457 nm, respectively). All of them showed blue emissions in THF solution, partially attributed to the twisted conformation. The results demonstrated that the minor difference of their electronic structure could not substantially affect their emissions in THF solution. Moreover, the PL lifetime ( $\tau$ ) and absolute fluorescence quantum yields ( $\Phi_F$ ) in THF solution (concentration= 10  $\mu$ M) were also recorded (Figure 2b and Table 1). **TPA-CHO**, **TPA-CHO-2F** and **TPA-CHO-2Cl** exhibited higher absolute fluorescence quantum yields of 28.06, 31.29 and 29.48 %, and longer lifetimes of 2.87, 3.06 and 2.50 ns, respectively (Fig. 2b), while **TPA-CHO-2Br** presented lower absolute fluorescence quantum yield of 8.72 % and shorter lifetime of 1.24 ns. Their photos under the illumination of a 365 nm UV lamp clearly showed their different fluorescence intensity under the same conditions. We could easily find that **TPA-CHO-2Br** presented weaker fluorescence luminescent intensity in comparison with the other TPA derivatives, well corresponding to their different absolute fluorescence quantum yields in THF solution. Additionally, radiative ( $k_r$ ) and non-radiative rates ( $k_{nr}$ ) in THF were calculated and presented in Table 1, confirming the fluorescence properties of these TPA derivatives. All of them possess similar radiative rates ( $0.98 \times 10^8$  s<sup>-1</sup> for **TPA-CHO**,  $1.02 \times 10^8$  s<sup>-1</sup> for **TPA-CHO-2F**,  $1.18 \times 10^8$  s<sup>-1</sup> for **TPA-CHO-2Cl**,  $0.7 \times 10^8$  s<sup>-1</sup> for **TPA-CHO-2Br**), which should be mainly attributed to the relatively high fluorescence efficiency in dilute THF solution. However, the nonradiative decay rate of **TPA-CHO-2Br** is  $7.36 \times 10^8$  s<sup>-1</sup>, much higher than that of other TPA derivatives ( $2.51 \times 10^8$  s<sup>-1</sup> for **TPA-CHO**,  $2.25 \times 10^8$  s<sup>-1</sup> for **TPA-CHO-2F**,  $2.82 \times 10^8$  s<sup>-1</sup> for **TPA-CHO-2Cl**). This indicated that the energy loss through nonradiative decay processes is

Table 1 Optical properties of **TPA-CHO** and **TPA-CHO-2X** (X= F, Cl, Br)

	$\lambda_{\text{abs max}}$ (nm)	$\lambda_{\text{em max}}$ (nm)	$\Phi_{\text{F}}$ (%)	$\tau_1$ (ns)	$\tau_2$ (ns)	$\tau_{\text{eve}}$ (ns)	$K_{\text{r}}^{[\text{a}]}$ ( $10^8 \text{ s}^{-1}$ )	$K_{\text{nr}}^{[\text{b}]}$ ( $10^8 \text{ s}^{-1}$ )
<b>TPA-CHO</b> (Solution)	354	468	28.06	2.00 (46.78)	3.63 (53.22)	2.87	0.98	2.51
<b>TPA-CHO</b> (Crystal)	–	454	40.45	1.1 (16.01)	2.84 (83.99)	2.56	1.58	2.32
<b>TPA-CHO</b> (Ground)	–	442	38.82	1.64 (53.04)	3.37 (46.96)	2.45	1.58	2.49
<b>TPA-CHO-2F</b> (Solution)	344	470	31.29	1.80 (45.34)	4.10 (54.66)	3.06	1.02	2.25
<b>TPA-CHO-2F</b> (Crystal)	–	460	56.07	2.16 (20.52)	6.32 (79.48)	5.47	1.03	0.80
<b>TPA-CHO-2F</b> (Ground)	–	458	57.85	2.59 (31.58)	6.57 (68.42)	5.31	1.09	0.79
<b>TPA-CHO-2Cl</b> (Solution)	353	459	29.48	1.80 (63.67)	3.73 (36.33)	2.50	1.18	2.82
<b>TPA-CHO-2Cl</b> (Crystal)	–	472	25.24	0.99 (61.89)	2.47 (38.11)	1.55	1.62	4.81
<b>TPA-CHO-2Cl</b> (Ground)	–	462	24.26	1.04 (55.90)	2.26 (44.10)	1.58	1.54	4.80
<b>TPA-CHO-2Br</b> (Solution)	353	457	8.72	0.94 (90.17)	4.00 (9.83)	1.24	0.70	7.36
<b>TPA-CHO-2Br</b> (Crystal)	–	470	11.21	0.63 (28.53)	1.45 (71.47)	1.22	0.92	7.30
<b>TPA-CHO-2Br</b> (Ground)	–	464	15.25	1.06 (53.04)	1.83 (28.98)	1.09	1.19	6.60

[a] The radiative rate ( $K_{\text{r}}$ ) can be obtained using equation  $K_{\text{r}} = \Phi_{\text{F}}/\tau$ .

[b]. The non-radiative rate ( $K_{\text{nr}}$ ) can be estimated from the equation  $\Phi_{\text{F}} = K_{\text{r}}/(K_{\text{r}}+K_{\text{nr}})$ .

enhanced after the introduction of bromine atoms to the **TPA-CHO**.<sup>[37]</sup>

To further investigate the emission behaviors of these four TPA derivatives in solid state, their single crystals were cultured by slow solvent evaporation of their solutions in the mixture solvents of dichloromethane and hexane, with the basic information summarized in Table S1. All of **TPA-CHO**, **TPA-CHO-2F**, **TPA-CHO-2Cl** and **TPA-CHO-2Br** possess twisted structures in crystal, and the average values of the torsion angles of **TPA-CHO**, **TPA-CHO-2F**, **TPA-CHO-2Cl** and **TPA-CHO-2Br** are 72.90°, 74.53°, 63.70° and 62.68°, respectively (Fig. S10). The one with smaller average values of the torsion angles possesses better conjugated structure, which could explain the molecular configuration dependent emission: the variation tendency of crystal emission (460 nm for **TPA-CHO-2F**, 472 nm for **TPA-CHO-2Cl**, 470 nm for **TPA-CHO-2Br**) is consistent with that of their average values of the torsion angles. In other words, the one with smaller average values of the torsion angles showed more redshifted emission in crystal state.<sup>[38]</sup> In comparison with **TPA-CHO-2Cl**, even though **TPA-CHO-2Br** possesses smaller torsion angle, it exhibits a little blue emission. On one hand, **TPA-CHO-2Cl** and **TPA-CHO-2Br** possess similar torsion angle, on the other hand, chlorine atoms has stronger electron withdrawing property than bromine atoms. Generally, the one with stronger electron withdrawing acceptor possesses redshifted emission. In consideration of those to two different effects, **TPA-CHO-2Br** showed blue-shifted emission compared to that of **TPA-CHO-2Cl**. Thanks to the twisted conformation of TPA block, which could prevent the possible  $\pi$ - $\pi$  stacking in solid state, **TPA-CHO**,

**TPA-CHO-2F** and **TPA-CHO-2Cl** possess high fluorescence efficiencies in crystal with high absolute fluorescence quantum yields of 40.45, 56.07 and 25.24 %, respectively) (Table 1). The lifetimes of crystals were also measured, with the values of 2.56, 5.47 and 1.55 ns, respectively (Fig. S11 and Table 1). Similar to the emission behavior in solution, **TPA-CHO-2Br** possess a lower fluorescence quantum yield (11.21 %) and shorter lifetime (1.22 ns) (Table 1 and Fig. S11). Additionally, radiative ( $k_{\text{r}}$ ) and non-radiative rates ( $k_{\text{nr}}$ ) in crystal were calculated and presented in Table 1, confirming the fluorescence properties of these TPA derivatives. All of them possess similar radiative rates ( $1.58 \times 10^8 \text{ s}^{-1}$  for **TPA-CHO**,  $1.03 \times 10^8 \text{ s}^{-1}$  for **TPA-CHO-2F**,  $1.62 \times 10^8 \text{ s}^{-1}$  for **TPA-CHO-2Cl**,  $0.92 \times 10^8 \text{ s}^{-1}$  for **TPA-CHO-2Br**), which should be mainly attributed to the relatively high fluorescence efficiencies in the crystal state. Their solid emission behaviors demonstrate that their high solid emissions are beneficial for their intense ML, mainly due to their twist structures.

When the crystalline samples of **TPA-CHO-2F** (CCDC 1883641), **TPA-CHO-2Cl** (CCDC 1883639) and **TPA-CHO-2Br** (CCDC 1883640) were scraped or ground at room temperature, intense blue ML emission could be discovered under the daylight (Fig. 1), indicating their unique ML effects. However, there was no ML signal observed for **TPA-CHO** (CCDC 1883638) when its crystal was scraped or ground even in dark. The ML spectrum of **TPA-CHO-F** presented only one peak at about 475 nm (Fig. 2c), which is coincided with the emission of **TPA-CHO-2F** in a THF solution. In consideration of the amorphous state of **TPA-CHO-2F** in a THF solution, the ML excited state of **TPA-CHO-2F** was more likely derived from the monomer situated at

the crystal surface when the crystal cracking under the mechanical stimulus. And ML spectra of **TPA-CHO-2Cl** (Fig. S12b) and **TPA-CHO-2Br** (Fig. S12c) were located at about 475 and 473 nm, according to their emission at crystal state. The different properties of those three TPA derivatives might be caused by the different molecular packing. The results demonstrated that the ML-inactive **TPA-CHO** was transferred to the ML-active materials after the introduction of halogen atoms. Considering the different response to the mechanical force, the patterns of their crystals under the mechanical stimulus should be carefully investigated.

Powder X-ray diffraction (PXRD) spectra in different states were measured to investigate the mechanochromism of these TPA-based ML luminogens (Fig. S13).<sup>[29]</sup> There were several strong diffraction peaks in the PXRD spectra of those four molecules in crystal state, due to the ordered packing in their crystals. After grinding lightly (pressure between 0.5 and 0.7 N, 3 mins), **TPA-CHO-2X** (X= F, Cl, Br) also exhibited strong peaks, and interestingly, even more peaks appeared as the result of the exposure of new generated crystal faces during the light grinding. The strong diffraction peaks indicated that **TPA-CHO-2X** (X= F, Cl, Br) maintained their crystal structures and the transformation to micro-crystals under the light grinding. Taking **TPA-CHO-2F** (Fig. 2d) as an example, the crystal **TPA-CHO-2F** exhibited apparent peaks at  $\theta = 10.2$  and  $21.5^\circ$ , indicating its good crystallinity. After grinding lightly, **TPA-CHO-2F** still showed sharp and intense diffraction peaks. Then further grinding heavily, **TPA-CHO-2F** also possessed strong peaks, implying the high rigidity of its crystals which could maintain its crystallinity to some extent upon the grinding. However, there are nearly no signals found in the PXRD spectrum of **TPA-CHO** after light grinding, demonstrating that the crystal structure of **TPA-CHO** was easily destroyed. Further grinding heavily (pressure between 1.7 and 1.9 N, 3 mins), there were still many sharp and strong peaks in the PXRD spectra of **TPA-CHO-2X** (F, Cl, Br), indicating that it was very hard to destroy their crystal structure and all of them retained their crystal structure to some extent.<sup>[33]</sup> As to **TPA-CHO**, there

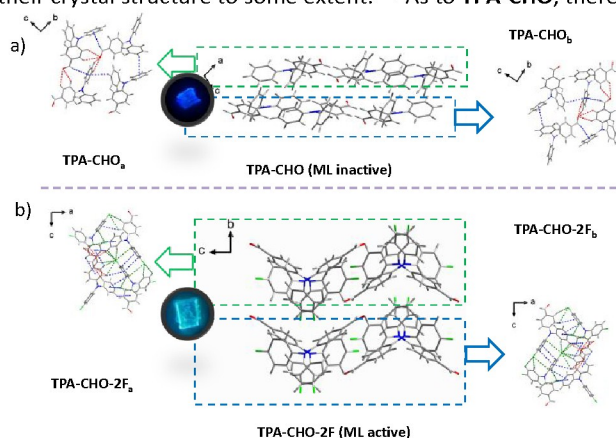


**Fig. 3** Crystal structure of **TPA-CHO** a) and **TPA-CHO-2F** b). Inset: The image of **TPA-CHO** and **TPA-CHO-2F** in crystal state under the illumination of a hand-held UV lamp ( $\lambda_{\text{exc}} = 360$  nm).

are no diffraction peaks, manifesting again that its crystal structure was totally destroyed. Thus, the rigidity of the **TPA-CHO-2X** (X=F, Cl, Br) crystal could efficiently suppress the possible nonradiative energy loss during the ML process.

To further study the latent reason of their different ML effects, the single crystals was thoroughly analyzed to explore the structure-packing-property relationship.<sup>[38]</sup> The space groups of **TPA-CHO**, **TPA-CHO-2F**, **TPA-CHO-2Cl** and **TPA-CHO-2Br** are  $P2(1)/c$ ,  $Pbca$ ,  $Pc$  and  $Pc$ , respectively (Table S2). The crystal cells of **TPA-CHO** and **TPA-CHO-2F** are centrosymmetric, while those of **TPA-CHO-2Cl** and **TPA-CHO-2Br** belong to non-centrosymmetric space groups, indicating their different molecular packing models. In comparison with that of **TPA-CHO**, after the modification with halogen atoms in **TPA-CHO-2F**, **TPA-CHO-2Cl** and **TPA-CHO-2Br**, the molecular packing changed as the results of their different electronic structures. As reported in literatures and our previous papers, the rigid molecular packing in crystal state could suppress the possible molecule slippage or collapse and restrain non-radiative pathway under the mechanical stimuli, which is necessary for the ML property.<sup>[26,27,29]</sup> Additionally, the intermolecular interactions have significant influences on the rigidity of crystal. Thus, intense intermolecular interactions play an important role for the mechanoluminescence.

To evaluate the intermolecular interactions in crystals, 8 molecules were selected, and only the intermolecular interactions shorter than  $4.0 \text{ \AA}$  were considered. The detailed results were summarized and presented in Fig. 3 and Table S3. In **TPA-CHO**, two different dimers were observed in the crystal, which could be named as **TPA-CHO<sub>a</sub>** and **TPA-CHO<sub>b</sub>** (Fig. 3a). For **TPA-CHO<sub>a</sub>**, there were 6 types of C-H...O bonds ranging from  $2.753$  to  $3.075 \text{ \AA}$ , and 4 types of C-H... $\pi$  bonds ranging from  $3.247$  to  $3.553 \text{ \AA}$  (Table S4). Similar intermolecular interactions for **TPA-CHO<sub>b</sub>** were also observed (Table S5). The interactions between **TPA-CHO<sub>a</sub>** and **TPA-CHO<sub>b</sub>** were summarized and listed in Table S12, including 4 types of C-H...O bonds with the distances of  $2.515 \text{ \AA}$ , 14 types of C-

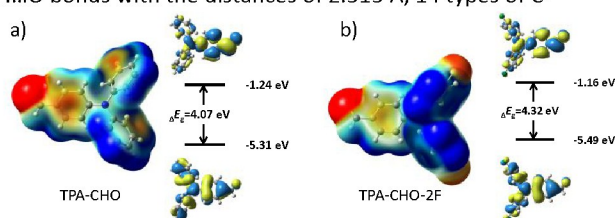


**Fig. 4** a) Electrostatic potential diagram and HOMO and LUMO of **TPA-CHO** a) and **TPA-CHO-2F**.

H... $\pi$  bonds with the distances ranging from  $3.071$  to  $3.877 \text{ \AA}$ . In comparison with the intermolecular interactions between **TPA-CHO<sub>a</sub>** and **TPA-CHO<sub>b</sub>**, those in **TPA-CHO<sub>a</sub>** and **TPA-CHO<sub>b</sub>** are much weaker. Under the mechanical stimulation, the weak intermolecular interactions of **TPA-CHO<sub>a</sub>** and **TPA-CHO<sub>b</sub>** could lead to non-radiative relaxation by molecular slippage or collapse at positions with weak intermolecular interactions, resulting in the ML-inactivity of **TPA-CHO**. When halogen atoms were introduced to **TPA-CHO**, intermolecular interactions were largely enhanced, due to the additional

interactions between halogen and hydrogen atoms. There were also two different types of dimers in the crystal of **TPA-CHO-2F**, **TPA-CHO-2F<sub>a</sub>** and **TPA-CHO-2F<sub>b</sub>**. As for **TPA-CHO-2F<sub>a</sub>**, there are 5 types of C-H...O bonds ranging from 2.462 to 3.886 Å, which are shorter than those of **TPA-CHO<sub>a</sub>**; 11 types of C-H... $\pi$  ranging from 3.466 to 3.978 Å as presented in Table S6, which are a little longer than those of **TPA-CHO<sub>a</sub>**; and 16 types of C-H...F (2.479 to 3.804 Å). The intermolecular interactions of **TPA-CHO-F<sub>b</sub>** (in Table S7) are as the same as those of **TPA-CHO-F<sub>a</sub>**. By analyzing the interactions between **TPA-CHO-F<sub>a</sub>** and **TPA-CHO-F<sub>b</sub>** (Table S13), 1 type of C-F...F-C (3.863 Å), 12 types of C-H...O bonds (2.915 to 3.966 Å), and 14 types of C-H...F bands (2.447 to 3.675 Å) could be easily observed. Similar intermolecular interactions could be found in crystals of **TPA-CHO-2Cl** and **TPA-CHO-2Br**, with detailed results listed in Fig 3, Table S8, Table S9, Table S10, Table S11, Table S14 and Table S15. All the results demonstrated that **TPA-CHO-2X** (X = F, Cl, Br) possesses much stronger intermolecular interactions rather than **TPA-CHO**. The intense intermolecular interactions of **TPA-CHO-2X** (X = F, Cl, Br) could enhance the crystal rigidities and impede the molecular slippage under the mechanical stimulus, thus resulting in their high-efficient ML emissions.<sup>[26-29]</sup>

To further reveal the relationships among molecular configuration, molecular electronic structure and ML performance, the highest occupied molecular orbitals (HOMO) and the lowest unoccupied molecular orbitals (LUMO) energy levels as well as the electrostatic potential (ESP) of the TPA derivatives were calculated, by using the density functional theory (DFT) calculation (Fig. 4 and Fig. S15). For **TPA-CHO**, the HOMO distributed over the TPA moiety and the LUMO mainly situated in the aldehyde group and neighboring benzene ring (Fig. 4a). As for **TPA-CHO-2F**, the HOMO and LUMO spread over the whole TPA (Fig. 4b), due to the electron withdrawing property of fluorine atoms. Similar distributions of the HOMO and LUMO levels were observed in **TPA-CHO-2Cl** and **TPA-CHO-2Br** (Fig. S15). Moreover, the negative electron areas (the red color area) of **TPA-CHO** located on the aldehyde group in

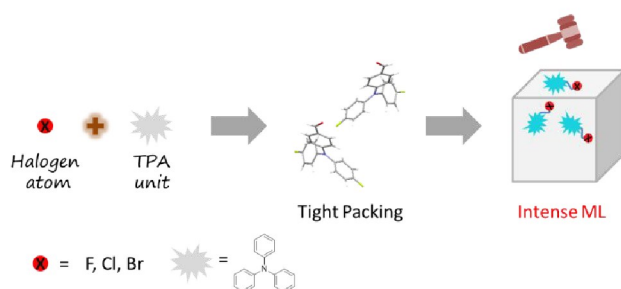


**Fig. 5** The strategy to construct bright ML materials with tight packing by introducing halogen atoms.

the ESP diagram (Fig. 4a). After the introduction of halogen atoms, the aldehyde group and halogen atoms both possessed abundant electrons. Additionally, the benzene ring substituted by halogen atoms showed more positive charges (Fig. 4 and Fig. S15). Considering the negative electron areas (the red color area: aldehyde group and halogen atoms), the strong interactions should occur between the negative and positive

electron areas (the blue color area: the aromatic hydrogen atoms located on the TPA block). Thus, the intermolecular interactions should be enhanced by introducing halogen atoms, similar to the results of the intermolecular interactions demonstrated in their single crystals. As reported previously by our group, strong intermolecular interactions play a significant role in realizing the ML property. **TPA-CHO-2F**, **TPA-CHO-2Cl** and **TPA-CHO-2Br** with stronger intermolecular interactions exhibit intense ML emission.<sup>[33-38]</sup> However, **TPA-CHO** which has weak intermolecular interactions is ML inactive. Strong intermolecular interactions could rigidify the molecules in crystal and then restrain the nonradiative energy losses by reducing molecular slippage under mechanical stimuli. By introducing halogen atom, the rigidity of **TPA-CHO-2X** (X = F, Cl, Br) are much-enhanced, due to changed electronic structures, the additional intermolecular interactions (such as C-H...X (X = F, Cl, Br), C-F...F-C) and enhanced intermolecular interactions (e.g., C-H... $\pi$  and C-H...O).<sup>[27]</sup> When the crystals of **TPA-CHO-2X** (X = F, Cl, Br) were fractured, enough excited energy was produced, due to the destruction of the strong intermolecular interactions (Fig. 5). Therefore, **TPA-CHO-2X** (X = F, Cl, Br) could emit intense ML signals under mechanical stimuli.

In consideration of their twist structure and relatively intense PL emission in solid state, the emission behaviors before and after grinding were also investigated.<sup>[35]</sup> **TPA-CHO** showed a blue-shifted emission from 454 nm (as-prepared state) to 442 nm (ground state) in Fig. S12a, which should be originated from the destruction of crystal structure to some extent and result in more twisted conformation. As reported in literatures, intermolecular interactions and molecular packing modes have significant influences on the emission of organic crystals. After grinding, the process of decreasing the intermolecular interactions could lead to the blue-shifted emission.<sup>[39a,39b]</sup> As shown in Fig. 3a, multiple weak intermolecular interactions, such as C-H...O and C-H... $\pi$  bonds, link the adjacent molecules to form dimer in **TPA-CHO<sub>a</sub>** and **TPA-CHO<sub>b</sub>**. After grinding, the molecular packing modes are disrupted and the dimers are broken due to the loss of the weak intermolecular interactions (C-H...O and C-H... $\pi$  bonds), leading to the blue-shifted emission. Similar blue-shifted emissions were observed after grinding the crystals of **TPA-CHO-2Cl** (Fig. S12b) and **TPA-CHO-2Br** (Fig. S12c). For **TPA-CHO-2Cl** and **TPA-CHO-2Br**, there were only 10 nm and 6 nm blue-shifted emissions after grinding. However, there is no apparent change for **TPA-CHO-2F** after grinding (Fig. 2c), the as-prepared powder of **TPA-CHO-2F** showed a blue emission (peak at 460 nm), however, after grinding, its emission exhibited almost no changes in the emission colour (peak at 458 nm). The insensitive response of **TPA-CHO-2F** is mainly due to the strong intermolecular interactions in the crystal which could effectively maintain its crystal structure after grinding. And the absolute fluorescence quantum yield and lifetimes of those TPA-based derivatives before and after grinding were also measured, without obvious changes observed. Using **TPA-CHO-2F** as an example, its crystal sample showed a high absolute fluorescence quantum yield of 56.07% and short life time of 5.47 ns, and, after grinding, its quantum yield and life time are 57.85% and

## ARTICLE

## Journal Name

5.31 ns, respectively. Those unchanged absolute fluorescence quantum yield and life time might be ascribed to the twisted structure of TPA moieties which could suppress the adverse  $\pi$ - $\pi$  stacking and maintain their high emission in solid state. The detailed optical properties before and after grinding were listed in Table 1.

## Conclusions

In summary, three halogen-substituted TPA derivatives with intense ML emission were designed and synthesized by introducing halogen atoms to the ML-inactive **TPA-CHO**, regardless of their similar PL emission in the solid state and analogous chemical structures. Detailed analysis of their crystal structures and theoretical calculations, demonstrated that the changed molecular electronic structure, which largely affected the intermolecular interactions and molecular packing in solid state, mainly contributed to their opposite ML effects. In other words, the introduction of halogen atoms is an efficient way to expand the ML family. Thus, the clear relationship among the molecular electronic structures, packing models in solid state and ML effects might provide an efficient guideline for the construction of pure organic materials with intense ML emission.

## Experimental section

### Materials and Characterization

Under an argon atmosphere, toluene was dehydrated and distilled from K-Na alloy. All the other reagents and chemicals were used as received, unless otherwise specified.  $^1\text{H}$  and  $^{13}\text{C}$  NMR spectra were recorded on a 400 MHz Varian Mercury spectrometer by using tetramethylsilane (TMS) as the internal standard. Mass spectra were carried out on a ZAB 3F-HF spectrometer. Elemental analyses were obtained on a RARIO EL III elemental analysis instrument. UV-Vis absorption spectra were performed on a Shimadzu UV-2550 Spectrophotometer. Photoluminescence (PL) spectra were conducted on a Hitachi F-4600 Fluorescence Spectrophotometer. Absolute PL quantum yields and PL lifetimes were obtained by using a FLS980 time-resolved spectrometer. ML spectrum was determined by using a spectrometer of Acton SP2750 with a liquid-nitrogen-cooled CCD (SPEC-10, Princeton) as a power detector in dark. D8 Advanced (Bruker) with Cu-K $\alpha$  radiation was utilized to record the X-ray powder diffraction (XRD) pattern. A Bruker Smart Apex CCD diffractometer was used to collect the single crystal XRD. And the crystals were cultured by slow evaporation of the solution in mixture solvents of n-hexane and DCM. The as-prepared samples were obtained by the treatment of rotary evaporation under the reduced pressure. All the TPA-based derivatives were prepared according to our reported literature.<sup>[40]</sup>

## Conflicts of interest

There are no conflicts to declare.

## Acknowledgements

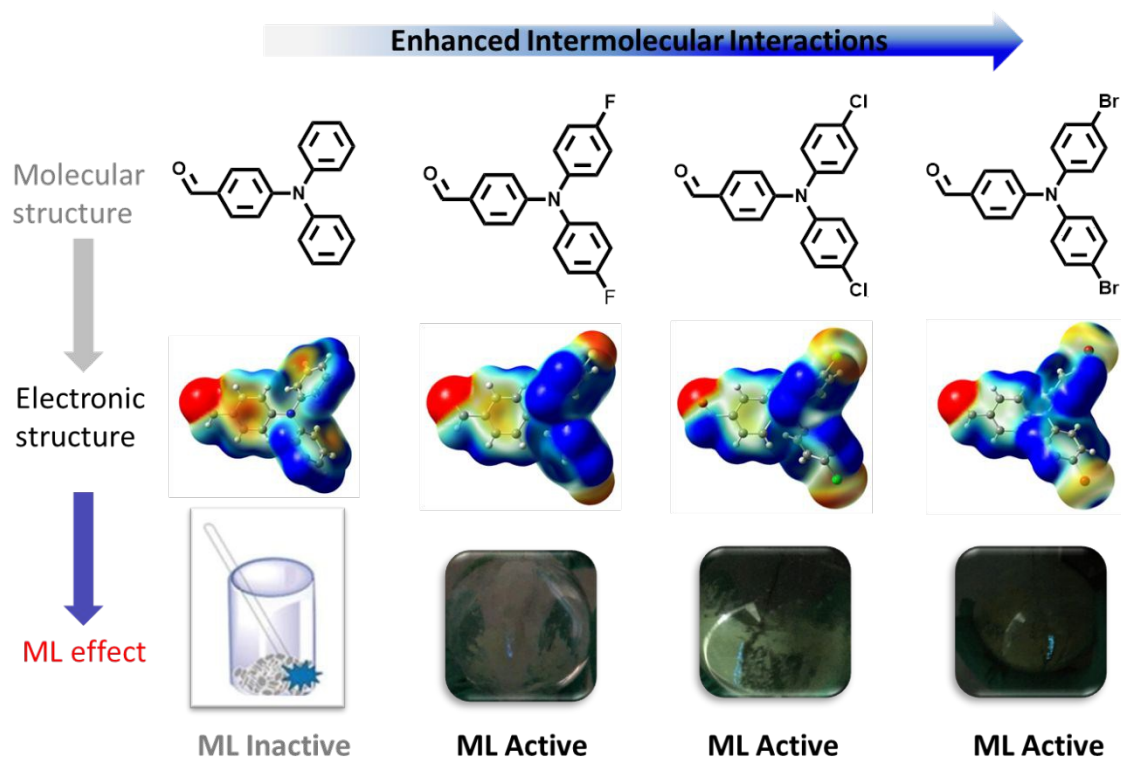
We are grateful to the National Natural Science Foundation of China (Nos. 51573140 and 21734007), Hubei Province (2017CFA002), and the Fundamental Research Funds for the Central Universities (2042017kf0247 and 2042018kf0014) for financial support.

## References

- 1 V. Merz and W. Weith, *Ber. Dtsch. Chem. Ges.*, 1873, **6**, 1511-1520.
- 2 J. Wang, K. Liu, L. Ma and X. Zhan, W. Weith, *Chem. Rev.*, 2016, **116**, 14675-14725.
- 3 M. Liang and J. Chen, *Chem. Soc. Rev.*, 2013, **42**, 3453-3488.
- 4 M. Ikai, S. Tokito, Y. Sakamoto and J. Chen, *Chem. Soc. Rev.*, 2013, **42**, 3453-3488..
- 5 P. Wu, C. He, J. Wang, X. Peng, X. Li, Y. An and C. Duan, *J. Am. Chem. Soc.*, 2012, **134**, 14991-14999.
- 6 N. Wu, M. Ng, V. Yam and B. Z. Tang, *Angew. Chem. Int. Ed.*, 2019, **58**, 3027-3031.
- 7 S. Wang, X. Yan, C. Cheng, H. Zhang, Y. Liu and Y. Wang, *Angew. Chem. Int. Ed.*, 2015, **54**, 13068-13072.
- 8 a) Y. Lin and X. Zhan, *Acc. Chem. Res.*, 2016, **49**, 175-183; b) P. Chen and Z. Li, *Chin. J. Polym. Sci.*, 2017, **35**, 793-798.
- 9 R. Li, W. Hu, Y. Liu and D. Zhu, *Acc. Chem. Res.*, 2009, **42**, 1719-1730.
- 10 J. Roncali, *Acc. Chem. Res.*, 2012, **45**, 1518-1528.
- 11 W. Li, Y. Pan, R. Xiao, Q. Peng, S. Zhang, D. Ma, F. Li, F. Shen, Y. Wang, B. Yang and Y. Ma, *Adv. Funct. Mater.*, 2014, **24**, 1609-1614.
- 12 W. Yuan, Y. Gong, S. Chen, X. Shen, J. W. Y. Lam, P. Lu, Y. Lu, Z. Wan, R. Hu, N. Xie, H. S. Kwok, Y. Zhang, J. Sun and B. Z. Tang, *Chem. Mater.*, 2012, **24**, 1518-1528.
- 13 a) H. Wang, Q. Yue, T. Nakagawa, A. Zieleniewska, H. Okada, K. Ogumi, H. Ueno, D. Guldi, X. Zhu and Y. Matsuo, *J. Mater. Chem. A*, 2019, **7**, 4072-4083; b) L. Feng, C. Wang, X. Deng, X. Miao, J. Wang, Y. Wang, Z. Li, *Mater. Chem. Front.*, 2018, **2**, 264-269. c) G. Huang, R. Wen, Z. Wang, B. Li, B. Z. Tang, *Mater. Chem. Front.*, 2018, **2**, 1884-1892; d) Y.-w. Wu, A.-j. Qin, B. Z. Tang, *Chin. J. Polym. Sci.*, 2017, **35**, 141-154.
- 14 C. Martin, C. Borreguero, K. Kennes, J. Hofkens, G. D. Miguel and E. M. Garia-Frutos, *Chem. Mater.*, 2019, **7**, 1222-1227.
- 15 H. Lu, K. Wang, B. Liu, M. Wang, M. Huang, Y. Zhang and J. Yang, *Mater. Chem. Front.*, 2019, **3**, 331-338.
- 16 C. Wu, B. Wang, Y. Wang, J. Hu, J. Jiang, D. Ma and Q. Wang, *J. Mater. Chem. C*, 2019, **7**, 558-566.
- 17 F. Ren, P. Liu, Y. Gao, J. Shi, B. Tong, Z. Cai and Y. Dong, *Mater. Chem. Front.*, 2019, **3**, 57-63.
- 18 G. Zhou, W.-Y. Wong, B. Yao, Z. Xie and L. Wang, *Angew. Chem. Int. Ed.*, 2007, **46**, 1149-1151.
- 19 X. Zhan, Z. Wu, Y. Lin, Y. Xie, Q. Peng, Q. Li D. Ma and Z. Li, *Chem. Sci.*, 2016, **7**, 4355-4363.
- 20 a) D. Luo, W. Yang, Z. Wang, A. Sadhanala, Q. Hu, R. Su, R. Shivanna, G. F. Trindade, J. F. Watts, Z. Xu, T. Liu, K. Chen, F. Ye, P. Wu, L. Zhao, J. Wu, Y. Tu, Y. Zhang, X. Yang, W. Zhang, R. H. Friend, Q. Gong, H. J. Snaith and R. Zhu, *Science*, 2018, **360**, 1442-1446; b) Y.-l. Liu, Z.-k. Wang, W. Qin, Q.-l. Hu, B. Z. Tang, *Chin. J. Polym. Sci.*, 2017, **35**, 365-371; c) Z. Qiu, B. Hao, X. Gu, Z. Wang, N. Xie, J. W.Y. Lam, H. Hao, B. Z. Tang, *Sci. China Chem.*, 2018, **6**, 966-970; d) Y. Zhou, H. Liu, N. Zhao, Z. Wang, M. Z. Michael, N. Xie, B. Z. Tang, Y. Tang, *Sci. China Chem.*, 2018, **61**, 892-897;
- 21 a) Y. Xie and Z. Li, *Chem*, 2018, **4**, 943-971; b) Y. Yuan, Y. Chen, *Chin. J. Polym. Sci.*, 2017, **35**, 1315-1327.
- 22 J. I. Zink, *Acc. Chem. Res.*, 1978, **11**, 289-295.

- 23 J. I. Zink, G. E. Hardy and J. E. Sutton, *J. Phys. Chem.*, 1976, **80**, 248-249.
- 24 Q. Yang, W. Wang, S. Xu and Z. L. Wang, *Nano Lett.*, 2011, **11**, 4012-4017.
- 25 C. Wang, B. Xu, M. Li, Z. Chi, Y. Xie, Q. Li and Z. Li, *Mater. Horiz.*, 2016, **3**, 220-225.
- 26 F. Liu, J. Tu, X. Wang, J. Wang, Y. Gong, M. Han, X. Dang, Q. Peng, Q. Li and Z. Li, *Chem. Commun.*, 2018, **54**, 5598-5601.
- 27 Y. Xie, J. Tu, T. Zhang, J. Wang, Z. Xie, Z. Chi, Q. Peng and Z. Li, *Chem. Commun.*, 2017, **53**, 11330-11333.
- 28 Z. Mao, Z. Yang, Y. Mu, Y. Zhang, Y.-F. Wang, Z. Chi, C.-C. Lo, S. Liu, A. Lien and J. Xu, *Angew. Chem. Int. Ed.*, 2015, **54**, 6270-6273.
- 29 J. Yang, Z. Ren, Z. Xie, Y. Liu, C. Wang, Y. Xie, Q. Peng, B. Xu, W. Tian, F. Zhang, Z. Chi, Q. Li and Z. Li, *Angew. Chem. Int. Ed.*, 2017, **56**, 898-902.
- 30 S. Xu, T. Liu, Y. Mu, Y.-F. Wang, Z. Chi, C.-C. Lo, S. Liu, A. Lien and J. Xu, *Angew. Chem. Int. Ed.*, 2015, **54**, 874-878.
- 31 J. Yang, X. Gao, Z. Xie, Y. Gong, M. Fang, Q. Peng, Z. Chi and Z. Li, *Angew. Chem. Int. Ed.*, 2017, **56**, 15299-15303.
- 32 a) J.-A. Li, J. Zhou, Z. Mao, Z. Xie, Z. Yang, B. Xu, C. Liu, X. Chen, D. Ren, H. Pan, G. Shi, Y. Zhang and Z. Chi, *Angew. Chem. Int. Ed.*, 2018, **57**, 6449-6453; b) C. Wang, Z. Li, *Mater. Chem. Front.* 2017, **1**, 2174-2194; c) C. Lin, R. Pan, P. Xing, B. Jiang, *Chin. J. Org. Chem.* 2018, **38**, 3260-3269; d) Q. Li, Y. Tang, W. Hu, Z. Li, *Small*, 2018, 1801560; e) J. Yang, Z. Chi, W. Zhu, B. Z. Tang, Z. Li, *Sci. China Chem.*, 2019, **62**, 1090-1098; f) Z. Li, *Sci. China Chem.*, 2017, **60**, 1107-1108; g) Y. Song, L. Zong, L. Zhang Z. Li, *Sci. China Chem.*, 2017, **60**, 1596-1601; h) Q. Z. Li, *Adv. Sci.*, 2017, **4**, 1600484; i) L. Zong, Y. Gong, Y. Yu, Y. Xie, G. Xie, Q. Peng, Q. Li, Z. Li, *Sci. Bulletin*, 2018, **63**, 108-116; j) Y. Xie, Z. Li, *Chem. Asian J.*, 2019, **14**, 2524-2541.
- 33 C. Wang, Y. Yun, Z. Chai, F. He, C. Wu, Y. Gong, M. Han, Q. Li and Z. Li, *Mater. Chem. Front.*, 2019, **3**, 32-38.
- 34 Y.-B. Gong, P. Zhang, Y.-R. Gu, J.-Q. Wangle, M.-M. Han, C. Chen, X.-J. Zhan, Z.-L. Xie, B. Zou, Q. Peng, Z.-G. Chi and Z. Li, *Adv. Optical Mater.*, 2018, **6**, 1800198.
- 35 M. Fang, J. Yang, Q. Liao, Y. Gong, Z. Xie, Z. Chi, Q. Peng, Q. Li and Z. Li, *J. Mater. Chem. C*, 2017, **5**, 9879-9885.
- 36 J. Wang, C. Wang, Y. Gong, Q. Liu, M. Han, T. Jiang, Q. Dang, Y. Li, Q. Li and Z. Li, *Angew. Chem. Int. Ed.*, 2018, **57**, 16821-16826.
- 37 J. Yang, X. Zhen, B. Wang, X. Gao, Z. Ren, J. Wang, Y. Xie, J. Li, Q. Peng, K. Pu and Z. Li, *Nat. Commun.*, 2018, **9**, 840.
- 38 J. Tu, F. Liu, J. Wang, X. Li, Y. Gong, M. Han, Y. Fan, Q. Li and Z. Li, *ChemPhotoChem*, 2019, **3**, 133-137.
- 39 a) Y. Lv, Y. Liu, X. Ye, G. F. Liu and X. T. Tao, *CrystEngComm*, 2015, **17**, 526-531; b) X. Cheng, Z. Wang, B. Tang, H. Zhang, A. Qin, J. Z. Sun and B. Z. Tang, *Adv. Funct. Mater.*, 2018, **28**, 1706506.
- 40 a) C.-W. Huang, F.-C. Chang, Y.-L. Chu, C.-C. Lai, T.-E. Lin, C.-Y. Zhu and S.-W. Kuo, *J. Mater. Chem. C*, 2015, **3**, 8142-8151; b) F. Liu, F. Wu, Z. Tu, Q. Liao, Y. Gong, L. Zhu, Q. Li and Z. Li, 2019, 201901296; c) Q. Fang and T. Yamamoto, *Macromolecules*, 2004, **37**, 5894-5899; d) Z. Chai, M. Wu, M. Fang, S. Wan, T. Xu, R. Tang, Y. Xie, A. Mei, H. Han, Q. Li and Z. Li, *Adv. Energy Mater.*, 2015, **5**, 1500846; d) Y. Fu, J. Yao, W. Xu, T. Fan, Q. He, D. Zhu, H. Cao and J. Cheng, *Polym. Chem.*, 2015, **6**, 20179-2182.

## TOC (Table of Contents)



Four TPA derivatives possess different ML effects due to the various electronic structures modulating by introducing of halogen atoms.